

# AdaSVD: Adaptive Singular Value Decomposition for Large Language Models

Anonymous ICCV submission

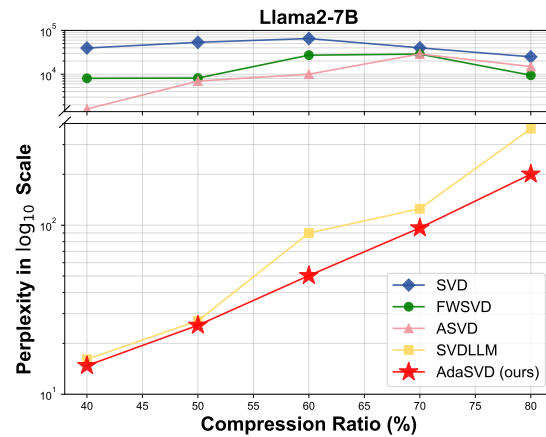
Paper ID 1059

## Abstract

**001** Large language models (LLMs) have achieved remarkable  
**002** success in natural language processing (NLP) tasks, yet  
**003** their substantial memory requirements present significant  
**004** challenges for deployment on resource-constrained devices.  
**005** Singular Value Decomposition (SVD) has emerged as a  
**006** promising compression technique for LLMs, offering consider-  
**007** able reductions in memory overhead. However, existing  
**008** SVD-based methods often struggle to effectively mitigate  
**009** the errors introduced by SVD truncation, leading to a no-  
**010** ticeable performance gap when compared to the original  
**011** models. Furthermore, applying a uniform compression ratio  
**012** across all transformer layers fails to account for the vary-  
**013** ing importance of different layers. To address these chal-  
**014** lenges, we propose AdaSVD, an adaptive SVD-based LLM  
**015** compression approach. Specifically, AdaSVD introduces **ada-**  
**016** **Comp**, which adaptively compensates for SVD truncation  
**017** errors by alternately updating the singular matrices  $\mathcal{U}$  and  
**018**  $\mathcal{V}^\top$ . Additionally, AdaSVD introduces **adaCR**, which adap-  
**019** tively assigns layer-specific compression ratios based on the  
**020** relative importance of each layer. Extensive experiments  
**021** across multiple LLM/VLM families and evaluation metrics  
**022** demonstrate that AdaSVD consistently outperforms state-of-  
**023** the-art (SOTA) SVD-based methods, achieving superior per-  
**024** formance with significantly reduced memory requirements.  
**025** We will release all the code and models of AdaSVD.

## 026 1. Introduction

027 Recently, large language models (LLMs) based on the Trans-  
028 former architecture [37] have shown remarkable potential  
029 across a wide range of natural language processing (NLP)  
030 tasks. However, their success is largely driven by their mas-  
031 sive scale, with models such as the LLaMA family [35] and  
032 the Open Pre-trained Transformer (OPT) series [45] con-  
033 taining up to 70B and 66B parameters, respectively. The  
034 substantial memory requirements of these models present  
035 significant challenges for deploying them on mobile devices.  
036 Consequently, the widespread adoption of LLMs remains  
037 limited by their immense resource demands [38, 39, 47].



**038** Figure 1. Comparison between vanilla SVD, FWSVD [17],  
**039** ASVD [42], SVD-LLM [40], and our AdaSVD on WikiText2.  
**040**

**041** Recent research on large language model (LLM) compres-  
**042** sion has explored various techniques, including weight quan-  
**043** tization [11, 22], network pruning [10, 34], low-rank fac-  
**044** torization [40, 42, 44], and knowledge distillation [15, 46].  
**045** Among these methods, low-rank factorization using Singu-  
**046** lar Value Decomposition (SVD) [17, 40, 42] stands out as a pow-  
**047** erful approach for reducing both model size and computa-  
**048** tional cost. SVD achieves this by decomposing large weight  
**049** matrices into smaller, low-rank components while preserv-  
**050** ing model performance. Since LLMs are often memory-  
**051** bound during inference [6, 7], SVD compression can effec-  
**052** tively accelerate model inference by reducing the memory  
**053** requirements, even when applied solely to the weights. This  
**054** approach does not require specialized hardware or custom  
**055** operators, unlike weight quantization, making SVD more  
**056** versatile across different platforms. Additionally, SVD is  
**057** orthogonal to other compression techniques [40], allowing  
**058** it to be combined with methods like weight quantization or  
**059** network pruning for even greater efficiency, enabling more  
**060** scalable and adaptable solutions for deploying LLMs.  
**061**

Recent advancements in SVD-based LLM compression, including FWSVD [17], ASVD [42], and SVD-LLM [40], have significantly improved the low-rank factorization approach, enhancing the overall effectiveness of SVD com-

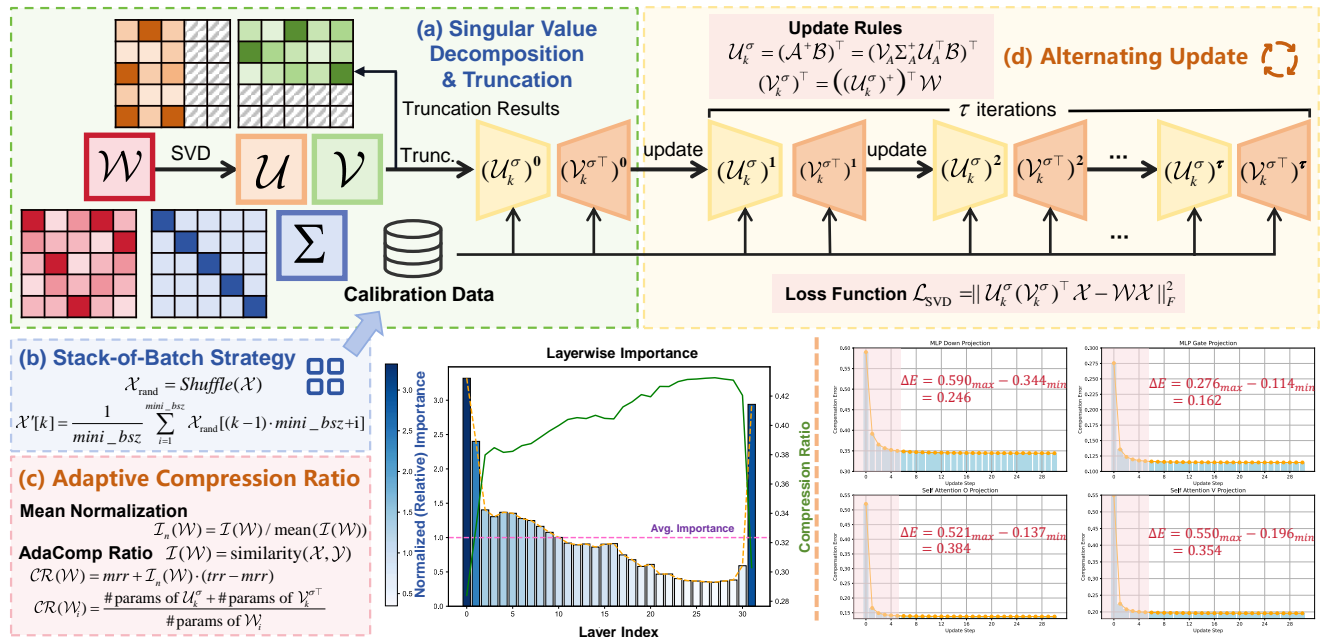


Figure 2. Overview of the proposed AdaSVD method: (a) SVD decomposition and truncation for linear layer weights; (b) Stack-of-batch strategy for efficient use of calibration data under limited GPU memory; (c) Adaptive compression ratio assignment (**adaCR**) based on layer-wise importance; (d) Adaptive compensation (**adaComp**) through alternating updates of  $\mathcal{U}$  and  $\mathcal{V}^\top$ .

pression. For example, FWSVD introduces Fisher information to prioritize the importance of parameters, while ASVD accounts for the impact of activation distribution on compression error. SVD-LLM establishes a relationship between singular values and compression loss through the data whitening techniques. While these methods have led to notable improvements in SVD compression, they still face challenges when applied at high compression ratios.

To bridge the performance gap between compressed and original models at both low and high compression ratios, we revisit SOTA solutions for LLM compression using SVD decomposition. Our analysis highlights two key observations: **First**, low-rank weight compensation after truncating the smallest singular vectors has been largely overlooked or insufficiently explored in prior methods. When truncating parts of the matrices  $\mathcal{U}$  and  $\mathcal{V}^\top$ , the remaining components should be adjusted accordingly to minimize the SVD compression error. **Second**, previous methods typically apply a uniform compression ratio across all transformer layers, failing to account for their varying relative importance. To address this, an importance-aware approach for assigning appropriate compression ratios is necessary.

To tackle the challenges outlined above, we propose AdaSVD, an adaptive SVD-based LLM compression method. **First**, AdaSVD proposes **adaComp**, an adaptive compensation technique designed to adjust the weights of  $\mathcal{U}$  and  $\mathcal{V}^\top$  after SVD truncation. By alternately updating the matrices  $\mathcal{U}$  and  $\mathcal{V}^\top$ , **adaComp** effectively reduces compression errors in a stable and efficient manner. To optimize the use of calibration data with limited GPU memory, we also intro-

duce a stack-of-batch technique when applying **adaComp**. **Second**, AdaSVD proposes **adaCR**, a method that assigns adaptive compression ratios to different layers based on their importance. With the target compression ratio fixed, this strategy significantly improves performance compared to using a uniform compression ratio across all layers.

Our key contributions are summarized as follows:

- We propose **adaComp**, a novel adaptive compensation method for SVD truncation. By alternately updating  $\mathcal{U}$  and  $\mathcal{V}^\top$  and employing the stack-of-batch technique, we effectively and stably minimize compression error.
- We propose **adaCR**, an adaptive compression ratio method that assigns layer-specific compression ratios according to their relative importance in LLMs. This importance-aware approach outperforms the previously used uniform compression ratio method.
- Extensive experiments on LLMs/VLMs demonstrate that our method, AdaSVD, significantly outperforms the previous SOTA SVD-based LLM compression method, SVD-LLM, effectively narrowing the performance gap between compressed and original models.

## 2. Related Works

### 2.1. LLM Compression Techniques

Recent advancements in model compression techniques have significantly enhanced the efficiency of deploying LLMs while maintaining their performance. Widely explored approaches include weight quantization [11, 22], network pruning [1, 10, 14, 25, 41], and hybrid methods [8]. In unstructured pruning, SparseGPT [10] prunes weights based on

062  
063  
064  
065  
066  
067  
068  
069  
070  
071  
072  
073  
074  
075  
076  
077  
078  
079  
080  
081  
082  
083  
084  
085  
086  
087  
088  
089  
090  
091  
092  
093  
094  
095  
096  
097  
098  
099  
100  
101  
102  
103  
104  
105  
106  
107  
108  
109  
110  
111  
112  
113  
114  
115  
116  
117  
118  
119  
120

**Algorithm 1** Pseudocode of AdaSVD

---

```

1: Inputs: LLM  $\mathcal{M}$ , Calib Data  $\mathcal{C}$ , Bucket Size  $M$ , Target Retention Ratio  $trr$ , Min Retention Ratio  $mrr$ , Update Iteration  $k$ 
2: Outputs: Updated Model  $\mathcal{M}'$  by AdaSVD
3: procedure ADASVD( $\mathcal{M}, \mathcal{C}, trr, mrr, k$ )
4:    $\mathcal{X} \leftarrow \text{GET\_CALIB}(\mathcal{C})$                                  $\triangleright$  Randomly collect samples as calibration data
5:    $\mathcal{X}'[1], \mathcal{X}'[2], \dots, \mathcal{X}'[M] \leftarrow \text{SOB}(\mathcal{X}, M)$        $\triangleright$  Shuffle samples and utilize stack-of-batch (SOB) strategy
6:    $\text{Set}_{\mathcal{S}} \leftarrow \text{WHITENING}(\mathcal{M}, \mathcal{X}')$ ,  $\text{Set}_{\mathcal{SVD}} \leftarrow \emptyset$ ,  $\text{Set}_{\mathcal{W}} \leftarrow \mathcal{M}$      $\triangleright$  Initialize sets of decomposed matrices and weights
7:    $\text{Set}_{\mathcal{CR}} \leftarrow \text{LAYER\_CR}(\mathcal{M}, \mathcal{X}', trr, mrr)$            $\triangleright$  Calculate layerwise importance and compression ratio
8:   for layer  $i$  in language model  $\mathcal{M}$  do
9:      $\mathcal{W}_i \leftarrow \text{Set}_{\mathcal{W}}(i)$ ,  $\mathcal{S}_i \leftarrow \text{Set}_{\mathcal{S}}(\mathcal{W}_i)$            $\triangleright$  Extract the whitening matrix of current weight  $\mathcal{W}_i$ 
10:     $\mathcal{U}_i, \Sigma_i, \mathcal{V}_i \leftarrow \text{SVD}(\mathcal{W}_i \mathcal{S}_i)$             $\triangleright$  Apply Singular Value Decomposition
11:     $\Sigma' \leftarrow \text{TRUNC}(\Sigma_i)$ ,  $(\mathcal{U}'_i, \mathcal{V}'_i) \leftarrow \text{TRUNC\_UV}(\mathcal{U}, \mathcal{V}, \Sigma')$      $\triangleright$  Apply adaptive compression ratio and truncation
12:     $\text{Set}_{\mathcal{SVD}} \leftarrow (\mathcal{U}'_i, \mathcal{V}'_i) \cup \text{Set}_{\mathcal{SVD}}$ 
13:   end for
14:    $\mathcal{M}' \leftarrow \text{ADA\_UPDATE}(\mathcal{M}, \mathcal{X}', \text{SET}_{\mathcal{SVD}}, k)$            $\triangleright$  Utilize alternate update for  $\mathcal{U}'_i, \mathcal{V}'_i$  with iteration  $k$ 
15:   return  $\mathcal{M}'$ 
16: end procedure

```

---

their importance, as determined by the Hessian matrix. However, it faces challenges in achieving optimal speedup, particularly due to hardware compatibility issues. Structured pruning methods, in contrast, are more hardware-friendly. LLM-Pruner [25] selectively removes non-critical coupled structures using gradient information. LaCo [41] introduces a layer-wise pruning strategy, where subsequent layers collapse into preceding ones. Gromov et al. [14] explores the effectiveness of basic layer-pruning techniques combined with parameter-efficient fine-tuning (PEFT). Additionally, SliceGPT [1] has pioneered post-training sparsification, emphasizing the importance of layer removal order for optimal performance. Quantization techniques offer another significant avenue for compression. GPTQ [11] applies layer-wise quantization and reduces quantization errors through second-order error compensation. AWQ [22] introduces activation-aware weight quantization, employing a scale transformation between weights and activations. Moreover, BiLLM [19] and ARB-LLM [21] achieve further compression to 1-bit while maintaining remarkable performance. More recently, STB-LLM [8] combines 1-bit quantization with pruning to achieve even greater memory reduction for LLMs. However, many of these compression techniques face challenges related to hardware compatibility, often requiring custom CUDA kernels [8] to enable real-time inference speedup.

**2.2. SVD-based LLM Compression**

Singular Value Decomposition (SVD) is a widely used technique for reducing matrix size by approximating a matrix with two smaller, low-rank matrices [13]. Although SVD-based methods have demonstrated potential in compressing LLMs, their full capabilities remain underexplored. Standard SVD typically focuses on compressing the original weight matrix without considering the significance of individual pa-

rameters, which can lead to considerable compression errors. To address this, Hsu et al. [18] introduced FWSVD, which incorporates Fisher information to weight the importance of parameters. However, this method requires complex gradient calculations, making it resource-intensive. Another limitation of standard SVD is the impact of activation distribution on compression errors. To mitigate this, Yuan et al. [42] proposed ASVD, which scales the weight matrix with a diagonal matrix that accounts for the influence of input channels on the weights. Subsequently, Wang et al. [40] introduced SVD-LLM, which establishes a connection between singular values and compression loss. This work demonstrates that truncating the smallest singular values after data whitening effectively minimizes compression loss. Despite these advancements, existing methods still exhibit significant accuracy loss at higher compression ratios and lack a comprehensive approach for compensating compressed weights after SVD truncation. Furthermore, most methods apply a uniform compression ratio across all transformer layers, overlooking the varying importance of different layers. AdaSVD seeks to address these limitations by proposing an adaptive compensation method (**adaComp**) and an importance-aware adaptive compression ratio method (**adaCR**).

**3. Method**

**Overview.** As illustrated in Figure 2, our AdaSVD integrates adaptive compensation for SVD truncation (**adaComp**) with an adaptive importance-aware compression ratio method (**adaCR**). In Sec. 3.1, we first describe how **adaComp** compensates for SVD truncation. Next, in Sec. 3.2, we detail how **adaCR** determines the compression ratio based on layer importance. The pseudocode of AdaSVD is shown in Algorithm 1, and pseudocodes for **adaComp** and **adaCR** are provided in the supplementary file.

154  
155  
156  
157  
158  
159  
160  
161  
162  
163  
164  
165  
166  
167  
168  
169  
170  
171  
172  
173  
174  
175  
176

177  
178  
179  
180  
181  
182  
183  
184  
185  
186

187

### 3.1. Adaptive Compensation for SVD Truncation

188 SVD compression first applies SVD decomposition for matrix  $\mathcal{W}$ , and then truncates the smallest singular values:  
189

$$190 \quad \mathcal{W} = \mathcal{U}\Sigma\mathcal{V}^\top \approx \mathcal{U}_k\Sigma_k\mathcal{V}_k^\top = \widehat{\mathcal{W}}, \quad (1)$$

191 where  $\Sigma_k$  indicates the retaining top-k largest singular values,  
192  $\mathcal{U}_k$  and  $\mathcal{V}_k^\top$  represent the corresponding retaining singular  
193 vectors. Moreover, the diagonal matrix  $\Sigma_k$  can be further  
194 absorbed into  $\mathcal{U}_k$  and  $\mathcal{V}_k^\top$  by

$$195 \quad \mathcal{U}_k^\sigma = \mathcal{U}_k\Sigma_k^{\frac{1}{2}}, \quad \mathcal{V}_k^\sigma = \mathcal{V}_k\Sigma_k^{\frac{1}{2}}, \quad (2)$$

$$196 \quad \widehat{\mathcal{W}} = \mathcal{U}_k\Sigma_k\mathcal{V}_k^\top = \mathcal{U}_k^\sigma(\mathcal{V}_k^\sigma)^\top. \quad (3)$$

197 The truncation of the smallest singular values minimizes  
198 the compression error with respect to  $\mathcal{W}$ , ensuring that  
199  $\|\mathcal{U}_k^\sigma(\mathcal{V}_k^\sigma)^\top - \mathcal{W}\|_F^2$  is minimized, which we refer to as the  
200 vanilla SVD method. However, this approach does not fully  
201 account for the practical effects of  $\mathcal{X}$ . To address this limitation,  
202 we introduce a more application-relevant metric for the  
203 SVD compression error, defined as follows:

$$204 \quad \mathcal{L}_{\text{SVD}} = \|\widehat{\mathcal{W}}\mathcal{X} - \mathcal{W}\mathcal{X}\|_F^2 \\ 205 \quad = \|\mathcal{U}_k^\sigma(\mathcal{V}_k^\sigma)^\top\mathcal{X} - \mathcal{W}\mathcal{X}\|_F^2. \quad (4)$$

206 Previous works [18, 40, 42] have made significant efforts  
207 to minimize  $\mathcal{L}_{\text{SVD}}$ . However, some of them involve com-  
208 plex and time-consuming preprocessing steps. Furthermore,  
209 they still face substantial challenges in effectively mitigat-  
210 ing the large errors that arise under high compression ratios,  
211 particularly when truncating 60% or more of the parameters.

212 To compensate for the error attributed to SVD truncation,  
213 we need to optimize the following objective:

$$214 \quad \mathcal{U}_k^\sigma, \mathcal{V}_k^{\sigma\top} = \arg \min_{\mathcal{U}_k^\sigma, \mathcal{V}_k^{\sigma\top}} \|\mathcal{U}_k^\sigma\mathcal{V}_k^{\sigma\top}\mathcal{X} - \mathcal{W}\mathcal{X}\|_F^2. \quad (5)$$

215 A straightforward approach is to compute the partial deriva-  
216 tives of the SVD compression objective with respect to  $\mathcal{U}_k^\sigma$   
217 and  $\mathcal{V}_k^{\sigma\top}$ , resulting in the following expressions (additional  
218 details can be found in the supplementary file):

$$219 \quad \frac{\partial \mathcal{L}_{\text{SVD}}}{\partial \mathcal{U}_k^\sigma} = 0 \\ 220 \quad \Rightarrow \mathcal{U}_k^\sigma = \mathcal{W}\mathcal{X}\mathcal{X}^\top\mathcal{V}_k^\sigma((\mathcal{V}_k^\sigma)^\top\mathcal{X}\mathcal{X}^\top\mathcal{V}_k^\sigma)^{-1}, \quad (6)$$

$$221 \quad \frac{\partial \mathcal{L}_{\text{SVD}}}{\partial \mathcal{V}_k^{\sigma\top}} = 0 \\ 222 \quad \Rightarrow \mathcal{V}_k^{\sigma\top} = ((\mathcal{U}_k^\sigma)^\top\mathcal{U}_k^\sigma)^{-1}(\mathcal{U}_k^\sigma)^\top\mathcal{W}. \quad (7)$$

223 However, this method involves computing the matrix inverse,  
224 which can lead to unstable updates and significant compres-  
225 sion errors, as shown in Figure 3 (a). To mitigate the issue  
226 of numerical instability, we propose a two-fold strategy to  
227 enhance the update quality of  $\mathcal{U}_k^\sigma$  and  $\mathcal{V}_k^{\sigma\top}$ .

228 **First**, the optimization objective for  $\mathcal{U}_k^\sigma$  is reformulated  
229 as a Least Squares Estimation (LSE) problem, where  $\mathcal{V}_k^{\sigma\top}\mathcal{X}$   
230 is treated as the input and  $\mathcal{W}\mathcal{X}$  as the output:

$$231 \quad \mathcal{U}_k^\sigma = \arg \min_{\mathcal{U}_k^\sigma} \|\mathcal{A}(\mathcal{U}_k^\sigma)^\top - \mathcal{B}\|_F^2, \quad (8)$$

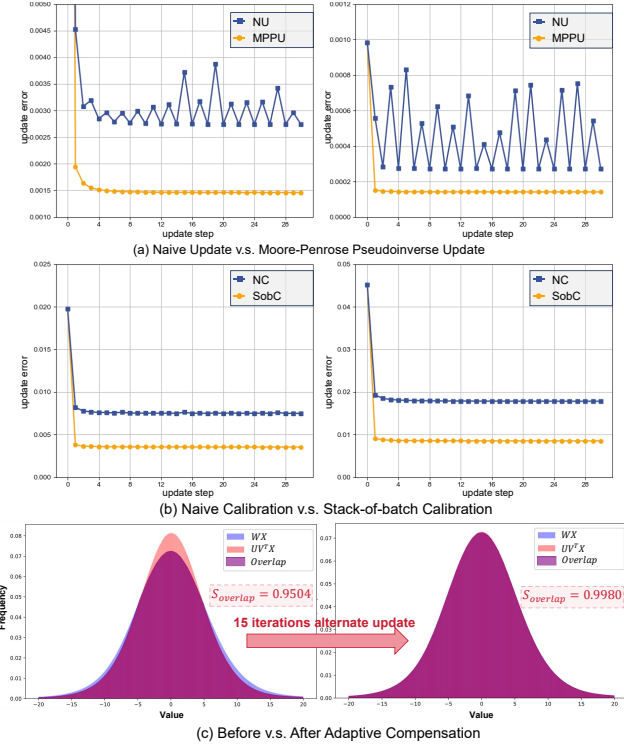


Figure 3. Adaptive compensation for SVD truncation (**adaComp**). (a) Comparison between naive (NU) and Moore-Penrose pseudoinverse update (MPPU). (b) Comparison between naive (NC) and stack-of-batch calibration strategy (SobC). (c) Distribution comparison before and after applying **adaComp**.

where  $\mathcal{A} = \mathcal{X}^\top\mathcal{V}_k^\sigma$  and  $\mathcal{B} = (\mathcal{W}\mathcal{X})^\top$ . Since  $\mathcal{A}$  is typically not a square matrix and may not be full rank, we first apply SVD to  $\mathcal{A}$  to enhance numerical stability:

$$232 \quad \mathcal{A} = \mathcal{U}_A\Sigma_A\mathcal{V}_A^\top, \quad (9)$$

and then obtain the solution for  $\mathcal{U}_k^\sigma$  by using the Moore-Penrose pseudoinverse [31] of  $\mathcal{A}$ :

$$233 \quad \mathcal{U}_k^\sigma = (\mathcal{A}^+\mathcal{B})^\top = (\mathcal{V}_A\Sigma_A^+\mathcal{U}_A^\top\mathcal{B})^\top, \quad (10)$$

where  $\Sigma_A^+$  denotes the Moore-Penrose pseudoinverse of  $\Sigma_A$ :

$$234 \quad \Sigma_A = \text{diag}(\sigma_1, \sigma_2, \dots, \sigma_n), \quad (11)$$

$$235 \quad \Sigma_A^+ = \text{diag}(\sigma_1^{-1}\mathbb{1}_{\sigma_1 \neq 0}, \sigma_2^{-1}\mathbb{1}_{\sigma_2 \neq 0}, \dots, \sigma_n^{-1}\mathbb{1}_{\sigma_n \neq 0}). \quad (12)$$

Similarly, we update  $\mathcal{V}_k^{\sigma\top}$  using the Moore-Penrose pseudoinverse of  $\mathcal{U}_k^\sigma$  to handle numerical instability:

$$236 \quad \mathcal{V}_k^{\sigma\top} = \arg \min_{\mathcal{V}_k^{\sigma\top}} \|\mathcal{U}_k^\sigma\mathcal{V}_k^{\sigma\top}\mathcal{X} - \mathcal{W}\mathcal{X}\|_F^2 \quad (244)$$

$$237 \quad = ((\mathcal{U}_k^\sigma)^+)^\top\mathcal{W}. \quad (13)$$

As shown in Figure 3 (a), by reformulating the optimization objective as an LSE problem and solving for  $\mathcal{U}$  and  $\mathcal{V}^\top$  using the Moore-Penrose pseudoinverse, we achieve a smooth curve that consistently reduces compression error stably.

**Second**, since the update rule incorporates the calibration data  $\mathcal{X}$ , ideally, a large volume of  $\mathcal{X}$  would yield better

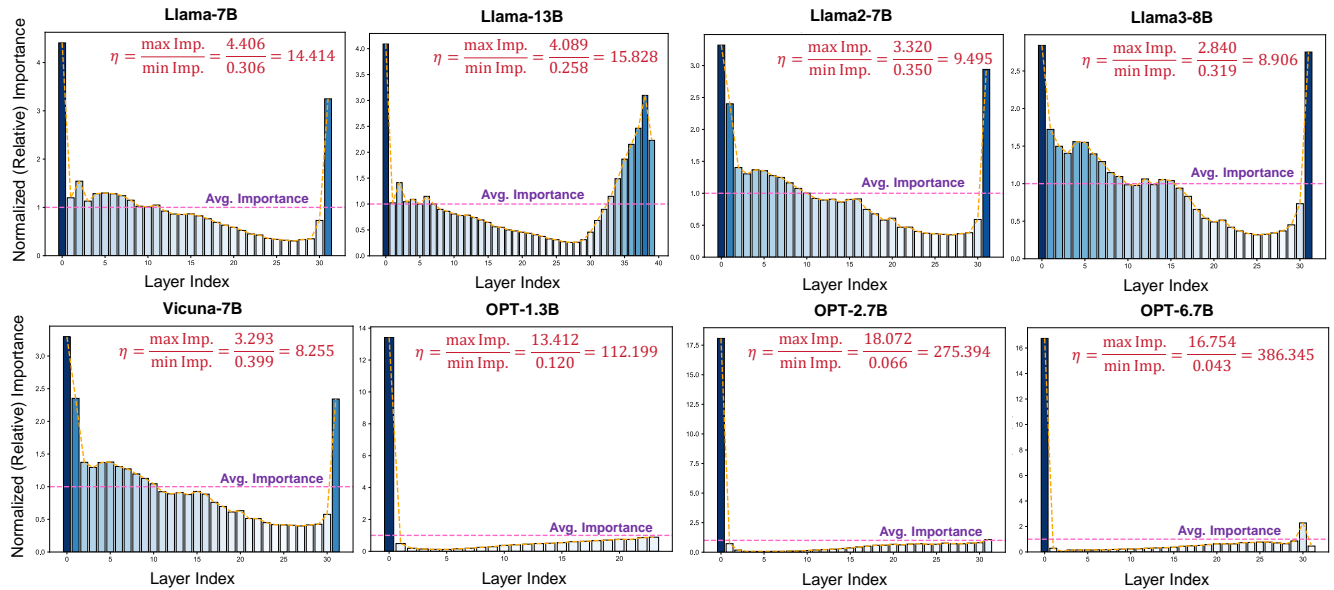


Figure 4. Layer-wise relative importance of different LLMs. The importance across different layers varies significantly, and the first layer always weight most importance. More layer-wise importance visualization can be found in the supplementary file.

results. However, during our experiments, we found that extending  $\mathcal{X}$  to just 32 samples on an 80GB GPU is challenging. To address this, we propose a **stack-of-batch** strategy that enables the utilization of more calibration data without increasing memory overhead. Specifically, given  $N$  calibration samples and a bucket size  $M$  (the maximum number of samples that can fit within the fixed GPU memory), we randomly sample  $mini\_bsz = \lceil \frac{N}{M} \rceil$  samples into one bucket by taking their mean value as follows:

$$\mathcal{X}_{\text{rand}} = \text{Shuffle}(\mathcal{X}), \quad (14)$$

$$\mathcal{X}'[k] = \frac{1}{mini\_bsz} \sum_{i=1}^{mini\_bsz} \mathcal{X}_{\text{rand}}[(k-1) \cdot mini\_bsz + i], \quad (15)$$

where  $k = 1, 2, \dots, M$ , and cardinality  $|\mathcal{X}'| = M$ . As shown in Figure 3 (b), integrating the **stack-of-batch** strategy further reduces the compression error.

As shown in Figure 2, to compensate for the error attributed to SVD truncation, we propose an adaptive method to subsequently update  $\mathcal{U}_k^\sigma$  and  $\mathcal{V}_k^\sigma$  with the above update rules. Moreover, the adaptation of  $\mathcal{U}_k^\sigma$  and  $\mathcal{V}_k^\sigma$  can be alternatively applied until convergence, where the update sequence over  $\tau$  iterations can be expressed as

$$\begin{aligned} (\mathcal{U}_k^\sigma)^1 &\rightarrow (\mathcal{V}_k^{\sigma \top})^1 \\ &\rightarrow (\mathcal{U}_k^\sigma)^2 \rightarrow (\mathcal{V}_k^{\sigma \top})^2 \\ &\rightarrow \cdots \rightarrow (\mathcal{U}_k^\sigma)^\tau \rightarrow (\mathcal{V}_k^{\sigma \top})^\tau, \end{aligned} \quad (16)$$

where  $(\mathcal{U}_k^\sigma)^\tau$  and  $(\mathcal{V}_k^{\sigma \top})^\tau$  denote the updated singular matrices after  $\tau$ -th iteration, respectively, while the region bounded by  $\boxed{\phantom{0}}$  corresponding to one iteration of alternative update. As shown in Figure 3 (c), the gap between the outputs of the compressed and original models narrows

after alternative updates. The overlapping area rapidly increases after just a few iterations. More visual comparisons are shown in the supplementary file.

Notably, our adaptive compensation can be integrated with data whitening proposed by Wang et al. [40] and Liu et al. [24], further reducing the SVD truncation error.

### 3.2. Adaptive SVD Compression Ratio

Previous studies on SVD compression typically apply a uniform compression ratio across all transformer layers of LLMs, overlooking the varying importance of different layers. Inspired by Men et al. [27] and Dumitru et al. [9], we propose **adaCR**, which adaptively determines the SVD compression ratio for each transformer layer, considering each layer's distinct impact on activations.

The importance of  $\mathcal{W}$  can be measured by its impact on the input, which is quantified as the similarity between the input  $\mathcal{X}$  and the output  $\mathcal{Y}$  after passing through  $\mathcal{W}$ .

$$\mathcal{Y} = \mathcal{W}\mathcal{X}, \quad (17)$$

$$\mathcal{I}(\mathcal{W}) = \text{similarity}(\mathcal{X}, \mathcal{Y}), \quad (18)$$

where  $\mathcal{I}(\mathcal{W})$  denotes the layer-wise importance of  $\mathcal{W}$ . The similarity metric used can vary, and for simplicity, we adopt cosine similarity in our method.

Then, we normalize  $\mathcal{I}(\mathcal{W})$  through mean centering to obtain the relative importance of  $\mathcal{W}$ :

$$\mathcal{I}_n(\mathcal{W}) = \mathcal{I}(\mathcal{W}) / \text{mean}(\mathcal{I}(\mathcal{W})). \quad (19)$$

After mean normalization, the average importance is 1. A value of  $\mathcal{I}_n(\mathcal{W})$  greater than 1 indicates greater importance, while a value lower than 1 indicates lesser importance. The compression ratio of each layer will be adaptively adjusted

RATIO	METHOD	WikiText-2↓	PTB↓	C4↓	Mmlu	ARC.e	WinoG.	HellaS.	PIQA	Average↑
0%	Original	5.68	8.35	7.34	45.30	74.62	69.22	76.00	79.11	68.85
40%	SVD	39,661.03	69,493.00	56,954.00	<b>26.51</b>	26.39	48.62	25.64	52.99	36.03
	FWSVD [18]	8,060.35	9,684.10	7,955.21	25.74	26.05	50.20	25.70	52.39	36.01
	ASVD [42]	1,609.32	7,319.49	1,271.85	24.35	26.81	49.49	25.83	53.81	36.06
	SVD-LLM [40]	16.11	719.44	61.95	22.97	36.99	56.04	30.49	56.96	40.69
AdaSVD		<b>14.76</b> (↓ 8%)	<b>304.62</b> (↓ 58%)	<b>56.98</b> (↓ 8%)	23.63	<b>41.12</b>	<b>58.17</b>	<b>31.75</b>	<b>58.49</b>	<b>42.63</b>
50%	SVD	53,999.48	39,207.00	58,558.00	<b>25.43</b>	25.80	47.36	25.55	52.67	35.36
	FWSVD [18]	8,173.21	8,615.71	8,024.67	24.83	25.84	48.70	25.64	52.83	35.57
	ASVD [42]	6,977.57	15,539.44	4,785.15	24.52	25.13	49.17	25.48	52.94	35.45
	SVD-LLM [40]	27.19	1,772.91	129.66	23.44	31.65	51.14	28.38	54.57	37.83
AdaSVD		<b>25.58</b> (↓ 6%)	<b>593.14</b> (↓ 67%)	<b>113.84</b> (↓ 12%)	23.24	<b>34.18</b>	<b>54.06</b>	<b>28.88</b>	<b>55.50</b>	<b>39.17</b>
60%	SVD	65,186.67	79,164.00	70,381.00	22.94	24.49	<b>51.85</b>	25.40	53.16	35.57
	FWSVD [18]	27,213.30	24,962.80	47,284.87	<b>26.91</b>	25.38	48.46	25.61	51.96	35.66
	ASVD [42]	10,003.57	15,530.19	9,983.83	26.89	26.68	48.86	25.76	51.80	36.00
	SVD-LLM [40]	89.90	2,052.89	561.00	22.88	26.73	47.43	26.89	<b>53.48</b>	35.48
AdaSVD		<b>50.33</b> (↓ 44%)	<b>1,216.95</b> (↓ 41%)	<b>239.18</b> (↓ 57%)	24.69	<b>28.20</b>	51.22	<b>27.36</b>	52.83	<b>36.87</b>

Table 1. Zero-shot performance comparison of LLaMA2-7B between AdaSVD and previous SVD compressed methods under 40% to 60% compression ratios. Evaluation on three language modeling datasets (measured by perplexity (↓)) and five common sense reasoning datasets (measured by both individual and average accuracy (↑)) demonstrate the effectiveness of AdaSVD.

METHOD	OPT-6.7B	LLaMA2-7B	Mistral-7B	Vicuna-7B
SVD	18,607.24	65,186.67	30,378.35	78,704.50
FWSVD [18]	8,569.56	27,213.30	5,481.24	8,185.66
ASVD [42]	10,326.48	10,003.57	22,705.51	20,241.17
SVD-LLM [40]	92.10	89.90	72.17	64.06
AdaSVD	<b>86.64</b> (↓ 6%)	<b>50.33</b> (↓ 44%)	<b>67.22</b> (↓ 7%)	<b>56.97</b> (↓ 11%)

Table 2. Perplexity (↓) of four different LLMs – OPT-6.7B, LLaMA2-7B, Mistral-7B, and Vicuna-7B – under 60% compression ratio on WikiText-2, where AdaSVD shows consistent improvements.

based on the relative importance:

$$\mathcal{CR}(\mathcal{W}) = mrr + \mathcal{I}_n(\mathcal{W}) \cdot (trr - mrr), \quad (20)$$

where  $mrr$  and  $trr$  are the minimum and target retention ratios, respectively. Notably,  $\mathcal{CR}(\mathcal{W}) = mrr$  when  $\mathcal{I}_n(\mathcal{W}) = 0$ , and  $\mathcal{CR}(\mathcal{W}) = trr$  when  $\mathcal{I}_n(\mathcal{W}) = 1$ .

Given the compression ratio for the  $i$ -th layer by **adaCR**, we truncate the vectors of least singular values from both  $\mathcal{U}_k^\sigma$  and  $\mathcal{V}_k^{\sigma\top}$  so that

$$\mathcal{CR}(\mathcal{W}_i) = \frac{\#\text{params of } \mathcal{U}_k^\sigma + \#\text{params of } \mathcal{V}_k^{\sigma\top}}{\#\text{params of } \mathcal{W}_i}. \quad (21)$$

As shown in Figure 4, the importance of different layers varies. It can be observed that the first layer always weighs the most importance, suggesting that we should retain more weight on it. For the Llama family, the relative importance curve approximates a bowl shape, highlighting the significance of both the initial and final layers.

## 4. Experiments

### 4.1. Setup

We compare our AdaSVD with four baselines, including vanilla SVD and SOTA SVD-based LLM compression methods FWSVD [18], ASVD [42], and SVD-LLM [40].

**Models and Datasets.** To demonstrate the generalizability

of our method, we evaluate the performance of AdaSVD and the baselines on four models from three different LLM families, including LLaMA2-7B [36], OPT-6.7B [45], Mistral-7B [20], and Vicuna-7B [4]. We benchmark on eight datasets, including three language modeling datasets (WikiText-2 [28], PTB [26], and C4 [32]) and five common-sense reasoning datasets (WinoGrande [33], HellaSwag [43], PIQA [2], ARC-e [5], and Mmlu [16]). We use the LM-Evaluation-Harness framework [12] to evaluate the model performance on these zero-shot Question-Answering (QA) datasets.

**Implementation Details.** To ensure a fair comparison, we followed ASVD [42] and SVD-LLM [40] to randomly select 256 samples from WikiText-2 as the calibration data and conduct data whitening before SVD truncation. All the experiments are conducted with PyTorch [30] and Huggingface [29] on a single NVIDIA A100-80GB GPU.

## 4.2. Main Results

We evaluate the overall performance of AdaSVD from three aspects: (1) performance under different compression ratios (**40%, 50%, 60%, 70%, and 80%**), (2) performance on different LLMs. (3) performance on visual language models. Some performance evaluation results and generated contents by the compressed LLMs are included in the supplementary file to provide a more straightforward comparison.

### Performance under Different Compression Ratios.

First, we evaluate the performance of LLaMA2-7B compressed by AdaSVD, vanilla SVD and the SOTA method SVD-LLM [40] under compression ratios ranging from 40% to 80% on all 8 datasets, as shown in Sec. 3.1. On the three language modeling datasets, AdaSVD consistently outperforms vanilla SVD, and SVD-LLM across all the compression ratios. More importantly, AdaSVD exhibits significant advantages over the baselines under higher compression ratios.



**SVD:** a man standing on one side of the road and another man sitting on the other side. In this book, it's was written by an author who wrote ...

**SVD-LLM:** Assistants - Asassstant - assasat - as - sasasm - saasam \u2013 Sasmas \u2013 Saas...

**AdaSVD:** The vehicle is a motorcycle, which is an automobile that is used for transportation. ...



**SVD:** it's a man ... and he has been injured by an injury that he was not able to play at 20 ...

**SVD-LLM:** a man who was seen to be an outsider, and he was not able to play at all, but he played with his right hand, which was broken, ...

**AdaSVD:** It's a person playing tennis on court, and he is wearing white shorts. ... playing his tennis with a tennis racket, ...



**SVD:** In this book, it's written by ... John an author of his own books and he is known for his writing ...

**SVD-LLM:** What'stans was an old name, used by a group of people who were on their way to city...

**AdaSVD:** It's a photo of children standing together, wearing uniforms... They are sitting on their knees, it is an old photograph that ...



**SVD:** ... The mountains are covered with snow, ... difficult for them to climb ... not able to walk through the snow ... trapped in snow holes

**SVD-LLM:** ... walking on snowy mountains, snow falls down from top of the mountain to bottom ...

**AdaSVD:** The mountain is covered by snow, ... a group of people skiing and walking on slopes.

Figure 5. We perform image captioning by applying SVD, SVD-LLM [40], and our AdaSVD to LLaVA-7B model on the COCO dataset respectively, highlighting the correct captions and wrong captions in different colors.

362 tios. These results indicate that AdaSVD is more effective in  
363 compressing LLMs for more resource-constrained devices  
364 such as smartphones and IoT devices, which often have  
365 limited memory and processing capabilities. On the five  
366 common sense reasoning datasets, AdaSVD also maintains  
367 its edge and performs better than the best-performing base-  
368 line on most of the datasets and consistently achieves higher  
369 average accuracy across all the compression ratios. Due to  
370 page limitations, comparisons for 70% and 80% compres-  
371 sion ratios are provided in the supplementary file.

372 **Performance on Different LLMs.** To demonstrate the  
373 generability of AdaSVD across different LLMs, we compare  
374 AdaSVD and the baselines on four different models OPT-  
375 6.7B, LLaMA2-7B, Vicuna-7B, and Mistral-7B – under  
376 60% compression ratio on WikiText-2. As shown in Tab. 2,  
377 AdaSVD consistently outperforms vanilla SVD, FWSVD,  
378 ASVD and SVD-LLM on all LLMs, and exhibits more  
379 stable performance across different LLMs, especially com-  
380 pared to vanilla SVD and FWSVD. We reproduce FWSVD,  
381 ASVD, and SVD-LLM using their official GitHub reposi-  
382 tories. FWSVD and ASVD fail on these LLMs with com-  
383 pression ratios under 60%, whereas SVD-LLM and AdaSVD  
384 maintain reasonable perplexity in such cases.

385 **Performance on Visual Language Models.** Note that  
386 our AdaSVD can also be applied to visual language models  
387 (VLMs) like LLaVA [23]. Following Lin et al. [22], we apply  
388 SVD compression to the language part of the VLMs since  
389 it dominates the model size. As shown in Figure 5, AdaSVD  
390 shows better image captioning results than vanilla SVD and  
391 SVD-LLM on COCO dataset [3] under 40% compression  
392 ratio. More image captioning comparisons with various  
393 compression ratios can be found in supplementary file.

### 394 4.3. Ablation Study

395 We provide extensive ablation study results in Tab. 3 to show  
396 the effect of some key components in our work.

397 **Effectiveness of Adaptive Compensation.** To validate  
398 the effectiveness of the proposed **adaComp**, we compare

399 the PPL results of Llama2-7B with and without **adaComp**  
400 on Wikitest-2, PTB, and C4 datasets in Tab. 3a. Results of  
401 70% and 80% compression ratios can be found in the sup-  
402 plementary file. It can be observed that AdaSVD consistently  
403 outperforms SVD-LLM after applying **adaComp**, and the  
404 performance gap is more significant under high compression  
405 ratios (*i.e.*, 60%, 70%, and 80%).

406 **Iteration Number.** To investigate the impact of the  
407 number of **adaComp** iterations under different compres-  
408 sion ratios, we perform an ablation study with 1, 3, and 15  
409 iterations, as shown in Tab. 3c. Results for 70% and 80%  
410 compression ratios are provided in the supplementary file. At  
411 lower compression ratios (*e.g.*, 40%, 50%, and 60%), it is ob-  
412 served that just 1 iteration of **adaComp** already outperforms  
413 the state-of-the-art method, SVD-LLM. However, increasing  
414 the number of iterations may lead to overfitting due to the  
415 limited calibration data, resulting in a performance drop. In  
416 contrast, at higher compression ratios (*e.g.*, 70% and 80%),  
417 additional iterations lead to performance improvements, in-  
418 dicating that AdaSVD is more effective in high compression  
419 ratio scenarios where previous methods still struggle. This  
420 highlights the importance of balancing the number of iter-  
421 ations with the available data to avoid over-optimization,  
422 especially in low compression scales.

423 **Effectiveness of Adaptive Compression Ratio.** To vali-  
424 date the effectiveness of our **adaCR**, we compared the results  
425 after removing **adaCR** (*i.e.*, using constant compression  
426 ratios for all layers) from AdaSVD. As shown in Tab. 3b,  
427 AdaSVD already outperforms SOTA SVD-LLM without us-  
428 ing **adaCR**, while integrating **adaCR** can further enhance  
429 the performance across all compression ratios.

430 **Minimum Retention Ratio.** The minimum retention  
431 ratio (*mrr*) in **adaCR** is also crucial, and we investigate the  
432 impact of different *mrr* values in Tab. 3d for 40%, 50%, and  
433 60% compression ratios (70% and 80% in supplemen-  
434 tary file). It can be observed that *mrr* remains relatively robust at  
435 lower compression ratios (40% and 50%), while contributing  
436 more at higher compression ratios (60%).

Method	Tgt. CR	adaComp	WikiText2 ↓	PTB ↓	C4 ↓
SVD-LLM	40%	✗	16.11	719.44	61.95
AdaSVD	40%	✗	15.47	406.83	66.29
AdaSVD	40%	✓	14.76	304.62	56.98
SVD-LLM	50%	✗	27.19	1,772.91	129.66
AdaSVD	50%	✗	30.00	1,101.15	166.02
AdaSVD	50%	✓	25.58	593.14	113.84
SVD-LLM	60%	✗	89.90	2,052.89	561.00
AdaSVD	60%	✗	78.82	6,929.39	339.31
AdaSVD	60%	✓	50.33	1,216.95	239.18

(a) Effectiveness of Adaptive Compensation

Method	Tgt. CR	CR	WikiText2 ↓	PTB ↓	C4 ↓
SVD-LLM	40%	Const	16.11	719.44	61.95
AdaSVD	40%	Const	15.38	617.11	60.43
AdaSVD	40%	Adapt	14.76	304.62	56.98
SVD-LLM	50%	Const	27.19	1,772.91	129.66
AdaSVD	50%	Const	27.33	1,177.53	126.85
AdaSVD	50%	Adapt	25.58	593.14	113.84
SVD-LLM	60%	Const	89.90	2,052.89	561.00
AdaSVD	60%	Const	69.46	2,670.20	336.90
AdaSVD	60%	Adapt	50.33	1,216.95	239.18

(b) Effectiveness of Adaptive Compression Ratio

Method	Tgt. CR	#Iteration	WikiText2 ↓	PTB ↓	C4 ↓
SVD-LLM	40%	-	16.11	719.44	61.95
AdaSVD	40%	1	14.76	304.62	56.98
AdaSVD	40%	3	15.47	249.41	57.28
AdaSVD	40%	15	15.84	257.96	57.39
SVD-LLM	50%	-	27.19	1,772.91	129.66
AdaSVD	50%	1	25.58	593.14	113.84
AdaSVD	50%	3	27.11	844.09	115.51
AdaSVD	50%	15	27.45	812.21	110.35
SVD-LLM	60%	-	89.90	2,052.89	561.00
AdaSVD	60%	1	50.33	1,216.95	239.18
AdaSVD	60%	3	64.12	3,546.45	301.19
AdaSVD	60%	15	62.34	4,293.79	267.29

(c) Iteration Number for Adaptive Compression

Table 3. Ablation studies on LLaMA-2-7B. Results are measured by perplexity, with best results highlighted in .

Method	Tgt. CR	MRR	WikiText2 ↓	PTB ↓	C4 ↓
SVD-LLM	40%	-	16.11	719.44	61.95
AdaSVD	40%	0.40	15.01	223.19	57.17
AdaSVD	40%	0.45	14.85	241.90	57.08
AdaSVD	40%	0.50	14.76	304.62	56.98
SVD-LLM	50%	-	27.19	1,772.91	129.66
AdaSVD	50%	0.40	25.58	593.14	113.84
AdaSVD	50%	0.45	26.01	814.63	117.58
AdaSVD	50%	0.50	27.33	1,177.53	126.85
SVD-LLM	60%	-	89.90	2,052.89	561.00
AdaSVD	60%	0.30	50.33	1,216.95	239.18
AdaSVD	60%	0.35	53.17	1,608.19	256.66
AdaSVD	60%	0.40	60.08	2,137.29	294.26

(d) Minimum Retention Ratio for Adaptive CR

RATIO	METHOD	GPTQ-INT4	WikiText-2↓	PTB↓	C4↓
0%	Original	✗	5.68	8.35	7.34
40%	SVD-LLM	✗	16.11	719.44	61.95
	SVD-LLM	✓	33.56	1,887.50	184.61
	AdaSVD	✗	14.76	304.62	56.98
	AdaSVD	✓	22.55	844.21	106.41
50%	SVD-LLM	✗	27.19	1,772.91	129.66
	SVD-LLM	✓	41.70	2,335.65	291.62
	AdaSVD	✗	25.58	593.14	113.84
	AdaSVD	✓	37.34	1,326.55	203.11
60%	SVD-LLM	✗	89.90	2,052.89	561.00
	SVD-LLM	✓	119.46	3,136.60	723.80
	AdaSVD	✗	60.08	2,137.28	294.26
	AdaSVD	✓	82.08	1,705.19	379.96
70%	SVD-LLM	✗	125.16	6,139.78	677.38
	SVD-LLM	✓	159.53	2,115.44	848.24
	AdaSVD	✗	107.90	5,027.62	441.33
	AdaSVD	✓	118.75	1,606.94	466.64
80%	SVD-LLM	✗	372.48	6,268.53	1,688.78
	SVD-LLM	✓	420.25	3,716.08	1,996.42
	AdaSVD	✗	206.51	6,613.44	679.66
	AdaSVD	✓	214.51	2,728.78	654.79

Table 4. AdaSVD with weight quantization method GPTQ.

#### 4.4. Integrate with Weight Quantization

Similar to previous SVD-based compression methods [17, 40, 42], our AdaSVD is orthogonal to other types of compression techniques. Following Wang et al. [40], we integrate AdaSVD with the widely used weight quantization method

GPTQ [11]. As shown in Tab. 4, we compare AdaSVD with SVD-LLM [40] on the LLaMA2-7B model, using different compression ratios (40%, 50%, 60%, 70%, and 80%) across the WikiText-2, PTB, and C4 datasets. The results demonstrate that, when combined with the 4-bit weight quantization method GPTQ, AdaSVD also consistently outperforms SOTA SVD-LLM across all compression ratios. Under high compression ratios (*i.e.*, 60%, 70%, and 80%), AdaSVD + GPTQ-INT4 even surpasses SVD-LLM.

## 5. Conclusion

In this work, we propose AdaSVD, an adaptive SVD-based compression method for LLMs. AdaSVD first proposes **adaComp**, which adaptively compensates for the error caused by the truncation of singular matrices, efficiently reducing compression error without requiring additional training. Furthermore, AdaSVD proposes **adaCR**, which adaptively assigns compression ratios based on the importance of each layer, further enhancing performance while maintaining the same target compression rate. Both strategies effectively minimize SVD compression errors, particularly at high compression ratios. Our experiments on multiple open-source LLM and VLM families demonstrate that AdaSVD pushes the performance boundary beyond the current state-of-the-art SVD-based LLM compression methods.

442  
443  
444  
445  
446  
447  
448  
449  
450  
451  
452  
453  
454  
455  
456  
457  
458  
459  
460  
461  
462  
463  
464  
465

466

## References

- [1] Saleh Ashkboos, Maximilian L. Croci, Marcelo Gennari do Nascimento, Torsten Hoefer, and James Hensman. Slicegept: Compress large language models by deleting rows and columns. In *ICLR*, 2024. 2, 3
- [2] Yonatan Bisk, Rowan Zellers, Ronan Le Bras, Jianfeng Gao, and Yejin Choi. Piqa: Reasoning about physical commonsense in natural language. In *AAAI*, 2020. 6
- [3] Xinlei Chen, Hao Fang, Tsung-Yi Lin, Ramakrishna Vedantam, Saurabh Gupta, Piotr Dollár, and C Lawrence Zitnick. Microsoft coco captions: Data collection and evaluation server. *arXiv preprint arXiv:1504.00325*, 2015. 7
- [4] Wei-Lin Chiang, Zhuohan Li, Zi Lin, Ying Sheng, Zhanghao Wu, Hao Zhang, Lianmin Zheng, Siyuan Zhuang, Yonghao Zhuang, Joseph E Gonzalez, et al. Vicuna: An open-source chatbot impressing gpt-4 with 90%\* chatgpt quality. In *LMSYS*, 2023. 6
- [5] Peter Clark, Isaac Cowhey, Oren Etzioni, Tushar Khot, Ashish Sabharwal, Carissa Schoenick, and Oyvind Tafjord. Think you have solved question answering? try arc, the ai2 reasoning challenge. *arXiv preprint arXiv:1803.05457*, 2018. 6
- [6] Tri Dao. Flashattention-2: Faster attention with better parallelism and work partitioning. In *ICLR*, 2024. 1
- [7] Tri Dao, Dan Fu, Stefano Ermon, Atri Rudra, and Christopher Ré. Flashattention: Fast and memory-efficient exact attention with io-awareness. In *NeurIPS*, 2022. 1
- [8] Peijie Dong, Lujun Li, Yuedong Zhong, Dayou Du, Ruibo Fan, Yuhan Chen, Zhenheng Tang, Qiang Wang, Wei Xue, Yike Guo, et al. Stbllm: Breaking the 1-bit barrier with structured binary llms. In *ICLR*, 2025. 2, 3
- [9] Razvan-Gabriel Dumitru, Paul-Ioan Clotan, Vikas Yadav, Darius Peteleaza, and Mihai Surdeanu. Change is the only constant: Dynamic llm slicing based on layer redundancy. In *EMNLP*, 2024. 5
- [10] Elias Frantar and Dan Alistarh. Sparsegept: Massive language models can be accurately pruned in one-shot. In *ICML*, 2023. 1, 2
- [11] Elias Frantar, Saleh Ashkboos, Torsten Hoefer, and Dan Alistarh. Gptq: Accurate post-training quantization for generative pre-trained transformers. In *ICLR*, 2023. 1, 2, 3, 8
- [12] Leo Gao, Jonathan Tow, Baber Abbasi, Stella Biderman, Sid Black, Anthony DiPofi, Charles Foster, Laurence Golding, Jeffrey Hsu, Alain Le Noac'h, Haonan Li, Kyle McDonell, Niklas Muennighoff, Chris Ociepa, Jason Phang, Laria Reynolds, Hailey Schoelkopf, Aviya Skowron, Lintang Sutawika, Eric Tang, Anish Thite, Ben Wang, Kevin Wang, and Andy Zou. A framework for few-shot language model evaluation. *Zenodo*, 2023. 6
- [13] G.H. Golub, Alan Hoffman, and G.W. Stewart. A generalization of the eckart-young-mirsky matrix approximation theorem. *Linear Algebra and its Applications*, 1987. 3
- [14] Andrey Gromov, Kushal Tirumala, Hassan Shapourian, Paolo Glorioso, and Daniel A. Roberts. The unreasonable ineffectiveness of the deeper layers. In *ICLR*, 2025. 2, 3
- [15] Yuxian Gu, Li Dong, Furu Wei, and Minlie Huang. Knowledge distillation of large language models. In *ICLR*, 2024. 1
- [16] Dan Hendrycks, Collin Burns, Steven Basart, Andy Zou, Mantas Mazeika, Dawn Song, and Jacob Steinhardt. Measuring massive multitask language understanding. *Proceedings of the International Conference on Learning Representations (ICLR)*, 2021. 6
- [17] Yen-Chang Hsu, Ting Hua, Sungjen Chang, Qian Lou, Yilin Shen, and Hongxia Jin. Language model compression with weighted low-rank factorization. In *ICLR*, 2022. 1, 8
- [18] Yen-Chang Hsu, Ting Hua, Sungjen Chang, Qian Lou, Yilin Shen, and Hongxia Jin. Language model compression with weighted low-rank factorization. In *ICLR*, 2022. 3, 4, 6
- [19] Wei Huang, Yangdong Liu, Haotong Qin, Ying Li, Shiming Zhang, Xianglong Liu, Michele Magno, and Xiaojuan Qi. Billm: Pushing the limit of post-training quantization for llms. In *ICML*, 2024. 3
- [20] Albert Q Jiang, Alexandre Sablayrolles, Arthur Mensch, Chris Bamford, Devendra Singh Chaplot, Diego de las Casas, Florian Bressand, Gianna Lengyel, Guillaume Lample, Lucile Saulnier, et al. Mistral 7b. *arXiv preprint arXiv:2310.06825*, 2023. 6
- [21] Zhiteng Li, Xianglong Yan, Tianao Zhang, Haotong Qin, Dong Xie, Jiang Tian, Linghe Kong, Yulun Zhang, Xiaokang Yang, et al. Arb-llm: Alternating refined binarizations for large language models. In *ICLR*, 2025. 3
- [22] Ji Lin, Jiaming Tang, Haotian Tang, Shang Yang, Wei-Ming Chen, Wei-Chen Wang, Guangxuan Xiao, Xingyu Dang, Chuang Gan, and Song Han. Awq: Activation-aware weight quantization for on-device llm compression and acceleration. 2024. 1, 2, 3, 7
- [23] Haotian Liu, Chunyuan Li, Qingyang Wu, and Yong Jae Lee. Visual instruction tuning. In *NeurIPS*, 2023. 7
- [24] Shih-Yang Liu, Huck Yang, Chein-Yi Wang, Nai Chit Fung, Hongxu Yin, Charbel Sakr, Saurav Muralidharan, Kwang-Ting Cheng, Jan Kautz, Yu-Chiang Frank Wang, et al. Eora: Training-free compensation for compressed llm with eigenspace low-rank approximation. *arXiv preprint arXiv:2410.21271*, 2024. 5
- [25] Xinyin Ma, Gongfan Fang, and Xinchao Wang. Llm-pruner: On the structural pruning of large language models. In *NeurIPS*, 2023. 2, 3
- [26] Mitch Marcus, Beatrice Santorini, and Mary Ann Marcinkiewicz. Building a large annotated corpus of english: The penn treebank. *CL*, 1993. 6
- [27] Xin Men, Mingyu Xu, Qingyu Zhang, Bingning Wang, Hongyu Lin, Yaojie Lu, Xianpei Han, and Weipeng Chen. Shortgpt: Layers in large language models are more redundant than you expect. *arXiv preprint arXiv:2403.03853*, 2024. 5
- [28] Stephen Merity, Caiming Xiong, James Bradbury, and Richard Socher. Pointer sentinel mixture models. In *ICLR*, 2017. 6
- [29] A Paszke, S Gross, F Massa, A Lerer, JP Bradbury, G Chanan, T Killeen, Z Lin, N Gimelshein, L Antiga, et al. An imperative style, high-performance deep learning library. In *NeurIPS*, 2019. 6

- 579 [30] Adam Paszke, Sam Gross, Francisco Massa, Adam Lerer,  
580 James Bradbury, Gregory Chanan, Trevor Killeen, Zeming  
581 Lin, Natalia Gimelshein, Luca Antiga, et al. Pytorch: An  
582 imperative style, high-performance deep learning library. In  
583 *NeurIPS*, 2019. 6
- 584 [31] R. Penrose. On the generalized inverse of matrices. *Mathe-*  
585 *matika*, 1955. 4
- 586 [32] Colin Raffel, Noam Shazeer, Adam Roberts, Katherine Lee,  
587 Sharan Narang, Michael Matena, Yanqi Zhou, Wei Li, and  
588 Peter J. Liu. Exploring the limits of transfer learning with a  
589 unified text-to-text transformer. *JMLR*, 2020. 6
- 590 [33] Keisuke Sakaguchi, Ronan Le Bras, Chandra Bhagavatula,  
591 and Yejin Choi. Winogrande: An adversarial winograd  
592 schema challenge at scale. *arXiv preprint arXiv:1907.10641*,  
593 2019. 6
- 594 [34] Mingjie Sun, Zhuang Liu, Anna Bair, and J Zico Kolter. A  
595 simple and effective pruning approach for large language  
596 models. In *ICLR*, 2024. 1
- 597 [35] Hugo Touvron, Thibaut Lavril, Gautier Izacard, Xavier Martinet,  
598 Marie-Anne Lachaux, Timothée Lacroix, Baptiste Rozière,  
599 Naman Goyal, Eric Hambro, Faisal Azhar, et al. Llama: Open and efficient foundation language models. *arXiv*  
600 *preprint arXiv:2302.13971*, 2023. 1
- 601 [36] Hugo Touvron, Louis Martin, Kevin Stone, Peter Albert, Am-  
602 ajad Almahairi, Yasmine Babaei, Nikolay Bashlykov, Soumya  
603 Batra, Prajjwal Bhargava, Shruti Bhosale, Dan Bikel, Lukas  
604 Blecher, Cristian Canton Ferrer, Moya Chen, Guillem Cu-  
605 curull, David Esiobu, Jude Fernandes, Jeremy Fu, Wenying  
606 Fu, Brian Fuller, Cynthia Gao, Vedanuj Goswami, Naman  
607 Goyal, Anthony Hartshorn, Saghar Hosseini, Rui Hou, Hakan  
608 Inan, Marcin Kardas, Viktor Kerkez, Madian Khabsa, Is-  
609 abel Kloumann, Artem Korenev, Punit Singh Koura, Marie-  
610 Anne Lachaux, Thibaut Lavril, Jenya Lee, Diana Liskovich,  
611 Yinghai Lu, Yuning Mao, Xavier Martinet, Todor Mihaylov,  
612 Pushkar Mishra, Igor Molybog, Yixin Nie, Andrew Poultion,  
613 Jeremy Reizenstein, Rashi Rungta, Kalyan Saladi, Alan Schel-  
614 ten, Ruan Silva, Eric Michael Smith, Ranjan Subramanian,  
615 Xiaoqing Ellen Tan, Bin Tang, Ross Taylor, Adina Williams,  
616 Jian Xiang Kuan, Puxin Xu, Zheng Yan, Iliyan Zarov, Yuchen  
617 Zhang, Angela Fan, Melanie Kambadur, Sharan Narang, Au-  
618 relien Rodriguez, Robert Stojnic, Sergey Edunov, and Thomas  
619 Scialom. Llama 2: Open foundation and fine-tuned chat mod-  
620 els. *arXiv preprint arXiv:2307.09288*, 2023. 6
- 621 [37] A Vaswani. Attention is all you need. In *NeurIPS*, 2017. 1
- 622 [38] Zhongwei Wan, Xin Wang, et al. Efficient large language  
623 models: A survey. In *TMLR*, 2023. 1
- 624 [39] Xin Wang, Zhongwei Wan, Arvin Hekmati, Mingyu Zong,  
625 Sамил Alam, Mi Zhang, and Bhaskar Krishnamachari. Iot in  
626 the era of generative ai: Vision and challenges. *IEEE Internet*  
627 *Computing*, 2024. 1
- 628 [40] Xin Wang, Yu Zheng, Zhongwei Wan, and Mi Zhang. Svd-  
629 llm: Truncation-aware singular value decomposition for large  
630 language model compression. In *ICLR*, 2025. 1, 3, 4, 5, 6, 7,  
631 8
- 632 [41] Yifei Yang, Zouying Cao, and Hai Zhao. Laco: Large lan-  
633 guage model pruning via layer collapse. In *EMNLP*, 2024. 2,  
634 3
- [42] Zhihang Yuan, Yuzhang Shang, Yue Song, Qiang Wu, Yan  
635 Yan, and Guangyu Sun. Asvd: Activation-aware singular  
636 value decomposition for compressing large language models.  
637 *arXiv preprint arXiv:2312.05821*, 2024. 1, 3, 4, 6, 8
- [43] Rowan Zellers, Ari Holtzman, Yonatan Bisk, Ali Farhadi, and  
638 Yejin Choi. Hellaswag: Can a machine really finish your  
639 sentence? In *ACL*, 2019. 6
- [44] Mingyang Zhang, Hao Chen, Chunhua Shen, Zhen Yang,  
640 Linlin Ou, Xinyi Yu, and Bohan Zhuang. Loraprune: Pruning  
641 meets low-rank parameter-efficient fine-tuning. In *ACL*, 2024.  
642 1
- [45] Susan Zhang, Stephen Roller, Naman Goyal, Mikel Artetxe,  
643 Moya Chen, Shuhui Chen, Christopher Dewan, Mona Diab,  
644 Xian Li, Xi Victoria Lin, et al. Opt: Open pre-trained trans-  
645 former language models. *arXiv preprint arXiv:2205.01068*,  
646 2022. 1, 6
- [46] Qihuang Zhong, Liang Ding, Li Shen, Juhua Liu, Bo Du, and  
647 Dacheng Tao. Revisiting knowledge distillation for autore-  
648 gressive language models. In *ACL*, 2024. 1
- [47] Zixuan Zhou, Xuefei Ning, Ke Hong, Tianyu Fu, Jiaming  
649 Xu, Shiyao Li, Yuming Lou, Luning Wang, Zhihang Yuan,  
650 Xiuhong Li, Shengen Yan, Guohao Dai, Xiao-Ping Zhang,  
651 Yuhang Dong, and Yu Wang. A survey on efficient inference  
652 for large language models. *arXiv preprint arXiv:2404.14294*,  
653 2024. 1
- [48] 654
- [49] 655
- [50] 656
- [51] 657
- [52] 658
- [53] 659
- [54] 660